Journal of Materials Chemistry B

Accepted Manuscript

ROYAL SOCIETY OF CHEMISTRY

www.rsc.org/materialsB

c(RGDfE) conjugated multi-Functional nanomedicine delivery system for targeted pancreatic cancer therapy

Jing Sun,[a,b] Dong-Hyun Kim,[b] Yang Guo,[b] Zhaogang Teng,[a] Yanjun Li,[a] Linfeng Zheng,[b] Zhuoli Zhang,[b] Andrew C. Larson,[b] Guangming Lu[a]

[a] Department of Medical Imaging, Jinling Hospital, School of Medicine, Nanjing University, Nanjing, Jiangsu Province, P.R. China;

[b] Department of Radiology, Northwestern University, Chicago, Illinois, US

ABSTRACT

Pancreatic cancer is one of the five most lethal malignancies and has a poor prognosis due to its abundant stromal barriers and lack of effective available therapies. Although gemcitabine has been used as a standard therapy for several decades, there has been little progress in improvement of the 5-year survive rate due to low targeting efficiency to the pancreatic cancer cells. To achieve targeted delivery of gemcitabine to pancreatic cancer cells, we have developed a c(RGDfE) [cyclic (Arg-Gly-Asp-D-Phe-Glu)] conjugated multi-functional nanomedicine delivery system composed of a magnetic core and mesoporous silica shell. These magnetic mesoporous nanoparticles demonstrated sufficient relaxivity properties for detection with magnetic resonance imaging (MRI). These c(RGDfE) peptide conjugated magnetic mesoporous silica nanoparticles [c(RGDfE)-pMMSNs] can target pancreatic cancer cells and increase cellular uptake in human pancreatic cancer cell lines that overexpress integrin $\alpha_v\beta_3$. Gemcitabine loaded c(RGDfE)-pMMSNs were most efficiently targeted to pancreatic cancer cells (BxPC-3). Growth-inhibition of the BxPC-3 cell line was achieved in a time dependent manner consistent with observed drug release behavior. Intracellular targeted gemcitabine delivery using c(RGDfE)-pMMSNs offers a promising approach for the treatment of pancreatic cancer.

INTRODUCTION

Pancreatic cancer is the fourth leading cause of cancer-related deaths in United States and the 5 year-survive rate is less than 6%. It is estimated that there will be 45,220 new cases and 38,460 deaths caused by pancreatic cancer in United States in 2013.[1] In the past 30 years, little progress has been made to improve the 5-year survival rate of patients with pancreatic cancer.[2] Less than 20% patients are suitable for the surgery resection,[2] but even after the successful resection with negative margins, local regional recurrences often occur and adjuvant chemotherapy or postoperative treatment is required.[3-8] Chemotherapy and radiotherapy remain the primary options. Chemotherapy alone or in combination with radiation, may benefit patients with advanced pancreatic cancer. Gemcitabine has been used as the standard therapy for patients with advanced pancreatic cancer for more than a decade but the response rate is only 24% and the median survival time is only 5.6-5.9 months.[9] Multiple clinical trials combining gemcitabine with other therapeutic agents have failed to show significant improvements in survival time.[10-14] One possible reason for the limited sensitivity and overall resistance to gemcitabine is the insufficient diffusion of gemcitabine into tumors after systemic administration. Intracellular delivery of gemcitabine may be necessary to improve therapeutic efficacy. The development of improved multi-functional drug delivery systems is urgently needed to permit intracellular delivery of gemcitabine.[15-19]

A number of nanocarriers have been investigated for drug delivery.[16, 19-26] Among these nanomaterials, mesoporous silica nanoparticles (MSNs) have attracted much attention due to large surface areas and pore volume, tunable pore sizes and biocompatibility.[27-29] MSNs can readily be functionalized with covalent bonds and electrostatic interactions[30, 31] to release drug payload in controlled manner.[32-38] Moreover, MSNs can be combined with superparamagnetic iron oxide (SPIO) nanoparticles to form multifunctional magnetic silica nanoparticles (MMSN) for magnetic resonance imaging (MRI) of targeted drug delivery. *In vivo* measurements of drug delivery should ideal permit patient-specific adjustments to treatment regimens (additional drug dosing and switch to alternative therapies as needed) as well as early prediction of therapeutic outcomes. Furthermore, MSN can be augmented with signaling molecules to increase the efficiency of cellular uptake within the targeted tumor tissues. In this study, we utilize a c(RGDfE) peptide targeting probe which binds to integrin $\alpha_v\beta_3$ expressed on pancreatic cancer cells. The integrin $\alpha_v\beta_3$ belongs to the cell adhesion receptors family and is over expressed on endothelial cells as well as many types of tumor

cells associate glioblastoma, breast, prostate, and pancreatic cancer.[39-41] Integrin expression is associated with tumor progression, invasion and metastasis, thus making integrins appealing targets for molecular imaging and therapeutic targeting. The integrin $\alpha_v\beta_3$ can bind with short peptides containing Arg-Gly-Asp (RGD) sequences. These RGD-containing peptides can specifically recognize the integrin $\alpha_v\beta_3$. RGD-containing peptides have been used as targeting agents for imaging and therapy.[42-44] Cyclic RGD peptides c(RGDfE) have a higher binding affinity compared to linear RGD sequences.[45-47] RGD peptide conjugated MMSNs [c(RGDfE)-pMMSNs] should permit tumor cell specific internalization *via* integrin-mediated endocytosis for subsequent intra-cellular release of gemcitabine from the loaded c(RGDfE)-pMMSNs. Active targeting is expected to efficiently increase intra-cellular gemcitabine delivery and reduce the side effects caused by the systemic chemotherapy. These magnetic nanoparticles should also serve as a MRI contrast agents to monitor the biodistribution of c(RGDfE)-pMMSNs for early predictions of therapeutic response. The purpose of this study was to develop this efficient multifunctional magnetic drug delivery system for MRI-monitor gemcitabine delivery to pancreatic cancer.

MATERIALS AND METHODS

Chemicals

Iron (III) chloride ($FeCl_3$), ammonium hydroxide (25%, wt), diethylene glycol (DEG), sodium hydroxide (NaOH), polyacrylic acid (PAA), tetraethyl orthosilicate (TEOS), 3-aminopropyl-trimethoxysilane (APTMS), cetyltrimethylammonium bromide (CTAB), ethanol (99.99%), 1-ethyl-3-(3-dimethylaminopropyl) carbodiimide(EDC), N-Hydroxysuccinimide (NHS), dimethyl sulfoxide (DMSO), 3-[4,5-Dimethylthiazol-2-yl]-2,5-diphenyltetrazolium bromide (MTT), hydrochloric acid (HCl, 37%, wt) and rhodamine B isothiocyanate (RITC) were purchased from Sigma-Aldrich (St. Louis, USA). Gemcitabine chloride salt was obtained from LC laboratories (MA, USA). COOH-PEG-SH (MW. 5K) was purchased from Laysan Bio (Arab, Al, USA). [4-(N-maleimidomethyl) cyclohexane-1-carboxylic acid 3-sulfo-N-hydroxy-succinimide ester sodium salt] (sulfo-SMCC) was purchased from Pierce (Thermo Scientific Inc., Rockford, IL, USA). The c(RGDfE) [cyclo(Arg-Gly-Asp-D-Phe-Glu)] peptides were purchased from Peptides International Inc. (Louisville, KY,USA). Milli-Q water was used in all experiments. All chemicals were used without further purification.

Synthesis of Magnetic Nanoclusters (MNCs)

The MNCs were synthesized using a modified hydrothermal reaction.[48, 49] Briefly, NaOH (50 mmol) was dissolved in DEG (20 ml). After being heated at 120 °C for 1 h under nitrogen, the solution was cooled and then kept at 70 °C as the stock solution. PAA (4 mmol), $FeCl_3$ (0.4 mmol) and DEG (17 ml) were mixed and heated to 220 °C under nitrogen with vigorous stirring to form a uniform solution. After 30 min, the stock solution (2 ml) was injected rapidly into the above solution and then the mixture was further heated for an additional 1 h. The obtained products were washed with a mixture of ethanol and distilled water several times and then dried in vacuum for storage.

Synthesis of NH_2-Magnetic Mesoporous Silica Nanoparticles (MMSNs-NH_2)

MNCs (25 mg) were dispersed into a mixture of ethanol (80 ml), H_2O (20 ml) and ammonia hydroxide (1 ml). TEOS (200 µl) was added to the solution under magnetic stirring to react for 6 h at room temperature (RT). The obtained products were washed and separated magnetically. Then the products were dispersed into a mixture of CTAB (200 mg), ethanol (60 ml), H_2O (80 ml), APTMS (50 µl) and NH_4OH (1 ml). After stirring for 30 min, TEOS (80 µl) was added into the mixture to further react for 6 h. The obtained products were dispersed in ethanol solution containing hydrochloric acid and heated at 60 °C for 3 h to remove the CTAB. The final products were separated and washed with ethanol and water and then dried in vacuum.

Functionalization of MMSNs with Peptides c(RGDfE) [c(RGDfE)-pMMSNs]

The MMSNs-NH_2 was further modified with PEG (pMMSNs). In brief, a mixture of COOH-PEG-SH (10 mg) and sulfo-SMCC (50 µmol) was added to 10ml PBS solution containing 20 mg pMMSNs-NH_2 and then the solution was stirred at RT for an additional 24 h. After being washed for several times, the particles (pMMSNs) were collected and dispersed in PBS solution. Next, c(RGDfE) peptides were conjugated onto the surface of COOH-pMMSNs. Specifically, c(RGDfE) (10 µmol) was dissolved in PBS solution followed by adding EDC (10 µmol) and NHS (25 µmol). After stirring at RT for 10 min, 10 ml of PBS solution containing 20 mg COOH-pMMSNs was added. The reaction continued at RT for an additional 24 h. To remove the excess EDC, NHS and RGD peptides, the obtained products [c(RGDfE)-pMMSNs] were washed with distilled water until there were no peptides detected in the supernatant (checked with UV/visible spectrometer). The final products were stored at 4 °C.

Characterization

Transmission electron microscopy (TEM) was used to characterize the size and structure of MNCs and MMSNs. TEM images were acquired using a FEI Tecnai Spirit G2 at 120 kV. The crystal structure, size, and magnetic properties of

the synthesized samples were characterized using an X-ray diffractometer (XRD; Scintag XDS-2000), and vibrating sample magnetometer (VSM; Model 7400, Lake Shore, Westerville, OH, USA). The mesoporous sizes were measured with a BET gas adsorption test (Tristar 3000, Micromeritics, Norcross, GA, USA). The zeta-potential changes of the samples were investigated with a Zetasizer Nano-S (Malvern, Herrenberg, Germany). Relaxivity measurements were performed to compare MNC r_2 value with the r_2 value of commercial iron oxide nanoparticles (Feraheme® which are similar in size to the synthesized iron oxide nanoparticles in our MNCs). Iron concentrations were determined using inductively coupled plasma mass spectroscopy (ICP-MS, Perkin Elmer, Waltham, MA, USA). MRI was performed using 7 Tesla scanner (Clinscan, Bruker, Billerica, MA, USA). Agarose phantoms (1%) containing various concentrations of MNCs or Feraheme were scanned using a T_2-weighted multi-echo (4 TEs ranging from 11 ms to 45 ms) fast spin-echo sequence (TR=1000 ms). T_2 values were calculated by fitting signal decay curves measured from regions of interest (ROIs) drawn within phantom images reconstructed at each TE (Image J**,** National Institutes of Health).

Gemcitabine Loading and Release Study

The synthesized particles c(RGDfE)-pMMSNs were dispersed into gemcitabine solution (5 mg/ml) and then the solution was stirred overnight at RT. The products were collected by washing and centrifugation. The supernatant solutions were collected for measurement of gemcitabine loading. These particles loaded with gemcitabine were dispersed into PBS solution (1 mg/ml, pH=7.2). 1 ml of the above solution was placed into a dialysis bag (Spectra/Por Float-A-Lyzer G2, 10 kDa MWCO, Spectrum Laboratories) and the bag was subsequently placed in a beaker containing PBS buffer (pH=7.2). The dissolution media was kept at 37°C and constantly stirred (100 rpm). At specific time points, 1 ml of the dissolution media was extracted and replaced with 1ml fresh PBS solution to keep the total media volume at 100 ml. The concentrations of released gemcitabine were determined by measuring OD values at wavelength of 275 nm using a SpectraMax® M5 Multi-Mode Microplate Reader (Molecular Devices, Inc., Sunnyvale, California, USA).

Cell Lines and Cell Culture

Three human pancreatic cancer cell lines BxPC-3, Panc-1 and CFPAC-1 were obtained from American Type Culture Collection (ATCC, Rockville, MD). All the cells were cultured separately in their required media according to ATCC guidelines: BxPC-3 was cultured in RPMI-1640 medium (Gibco, Invitrogen Co., Grand Island, NY, US) supplemented

with 10% FBS, Panc-1 was cultured in DMEM medium (Gibco, Invitrogen Co., Grand Island, NY, US) supplemented with 10% FBS, and CFPAC-1 cells were cultured in Iscove's Modified Dulbecco's Medium (Lonza Inc., NJ, USA) containing 20% FBS. All cells were incubated at 37°C with 5% CO_2 and 95% humidity.

Cellular Targeting and Uptake

The cellular uptake of c(RGDfE)-pMMSNs was confirmed with a confocal fluorescence microscope (Carl Zeiss LSM 510 UVMETA, Thornwood, NY). The expression of Integrin $\alpha_v\beta_3$ in three pancreatic cancer cell lines (BxPC-3, Panc-1, CFPAC-1) was compared using immune fluorescence (IF) imaging and FITC labeled integrin $\alpha_v\beta_3$ antibodies. To study endocytosis of these particles in the different cell lines, the cells were seeded onto glass cover slides and incubated with either pMMSNs or c(RGDfE)-pMMSNs loaded with RITC for 24 h. Then all particles were removed and the cells were rinsed three times with PBS solution. The cells were fixed in 4% formaldehyde solution for 10 min and stained with DAPI. The samples were excited separately with lasers at different wavelengths (364 nm-blue, 488 nm-green and 543 nm-red) for multi-color fluorescent imaging. Samples for TEM imaging were prepared with similar methods to those used to prepare IF samples. BxPC-3 cells were incubated with c(RGDfE)-pMMSNs for 24 h. These cells were fixed in TEM fixative and embedded. MRI studies were also performed. The three different cell lines were incubated with pMMSNs (100 ug/ml) for different time periods (1, 8 and 24 h) and T2 weighted MR images were acquired to observe uptake efficiency of pMMSNs in each cell suspension (3-million cells within 2mL agar). MRI scans were performed using a 7 T MR scanner (Bruker Clinscan). T_2-weighted images were obtained with a repetition time (TR) and echo (TE) time of TR/TE = 3,000 ms/44 ms. All sequences were acquired with a field of view of 35 × 35 mm, a matrix of 256 × 256 pixels, turbo factor of 12, and slice thickness of 0.4 mm.

Evaluation of Therapeutic Efficacy

The cytotoxicity of pMMSNs upon exposure to three human pancreatic cancer cell lines (BxPC-3, CFPAC-1 and Panc-1) was assessed through MTT assay. Cells plated in 96-well plates (10^4 cells /100 µl) were first cultured for 24 h and then exposed to increasing concentrations of pMMSNs (0, 5, 10, 20, 40, 60, 80, 100 µg/ml) for another 72 hours. The cell viability was calculated using following formula (A=absorbance):

$$\text{Cell viability (\%)} = \left[\frac{(\overline{A_{sample}} - \overline{A_{blank}})}{(\overline{A_{control}} - \overline{A_{blank}})}\right] \times 100\%$$

The half-maximum inhibition concentration (IC_{50} value) of free gemcitabine was evaluated in three cell lines similar to the cytotoxicity experiment. The dose concentrations of gemcitabine were 0.00, 0.01, 0.10, 1.00, 10.00, 100.00 μM. To assess the therapeutic efficacy of c(RGDfE)-pMMSNs, MTT assays were performed using each of the three cell lines. Cells were co-cultured with c(RGDfE)-pMMSNs (20 μg/ml) for increasing time intervals. The resulting cell viabilities at different time points (1h, 8h, 24h) were calculated using the above formula.

RESULTS

Synthesis and Characterization of MNCs and MMSNs

7 nm iron oxide nanoparticles formed clusters when coupled with the polyacrylic acid [50]. The average size of the MNCs was 24 nm. These MNCs were water dispersible and stable in aqueous solution with a surface charge of −48.7 mV (zeta potential). The iron oxide magnetic nanoclusters were encapsulated within a porous silica shell to form magnetic drug carriers (**Fig. 1**). CTAB was used as the pore-generating template, which would be removed later to form the meso-structured silica shell. TEM images showed structures and sizes of the pMMSNs. These pMMSNs were uniformly spherical with average diameter of roughly 50 nm and a mesostructured silica shell of 15nm (**Fig. 2a**). 2-3 nm pores are shown within TEM image in **Fig. 2a** (right panel). The BET surface area of the etched silica shell encapsulated magnetic nanoclusters was 86 m^2/g, which was increased from the 14.7 m^2/g area of non-etched silica shell encapsulated magnetic nanoclusters. The X-ray diffraction pattern of the synthesized pMMSNs was consistent with our previous report [49] for crystalline magnetic silica nanoparticles (**Fig. 2b**). These drug carriers including silica and magnetic nanoclusters demonstrated a magnetization saturation of 27 emu/g. At 300 K, hysteresis behavior disappeared; these drug carriers exhibited superparamagnetic behavior with no coercivity or remanence (**Fig. 2c**). Surface modification of these nanoparticles was verified with measurements of zeta potential. The strong negative zeta potential (−48.7 mV) of the magnetic nanoclusters was changed to +20 mV by the amine modified mesoporous silica coating. Further, COOH-PEG-SH modification and biofunctionalization with c(RGDfE) peptides was confirmed with −14 mV and +18 mV of zeta potential, respectively (**Fig. 2d**). The MRI contrast effects of these pMMSNs were compared to commercial SPIOs with comparison of resulting T_2 relaxivities. T_2-weighted phantoms images are shown in **Fig. 3** (a: commercial SPIOs, b: synthesized pMMSNs). The signal intensity (SI) of these T_2-weighted images decreased with the increasing iron concentrations (0, 0.05, 0.10, 0.15, 0.20, 0.25 mM). These signal decreases were significantly greater for phantoms containing pMMSNs than for phantom containing comparable concentration levels

of SPIOs ($p<0.05$, **Fig. 3c**). The r_2 relaxivity of our pMMSNs (250.7 ±15.6 $mM^{-1} s^{-1}$) was two times greater than the measured r_2 relaxivity of the commercially available SPIOs (113.6 ± 13.3 $mM^{-1} s^{-1}$) (**Fig. 3c**).

Cellular Uptake

The amount of c(RGDfE) peptides conjugated onto the surface of pMMSNs was approximately 0.2014 μmol / mg [c(RGDfE) conjugated amount (μmol) pMMSNs amount (mg)]. pMMSN or c(RGDfE)-pMMSN loaded with RITC were used to compare cellular uptake in three human pancreatic cancer cell lines. The results for these studies are shown in **Fig. 4**. For pMMSNs, there was relatively minimal observed uptake for each of the three cell lines (**Fig. 4**. **iv-vi**). However, the uptake of c(RGDfE)-pMMSN in BxPC-3 cells was much higher; this observed c(RGDfE)-pMMSN uptake in BxPC-3 cells was greater than that observed in the Panc-1 and CFPAC-1 cell lines (**Fig. 4. vii-ix**). This result was consistent with the elevated expression of integrin $\alpha_v\beta_3$ in the BxPC-3 cell line compare to Panc-1 and CFPAC-1 cell lines (**Fig. 4. i-iii**). TEM imaging was also performed to further confirm the cellular uptake of c(RGDfE)-pMMSNs in BxPC-3 cells. TEM results are shown in **Fig. 5** with a large number of intra-cellular c(RGDfE)-pMMSNs aggregated around the nucleus (**Fig. 5. a, b**).

MRI Studies

T_2-weighted MR images of cell suspension phantoms are included in **Fig. 5.c**. These images and accompanying signal intensity measurements demonstrated marked reductions in signal intensity after incubation with c(RGDfE)-pMMSNs with the greatest reduction observed after 24 hours. Signal reductions were strongest for the BxPC-3 cells and weakest for Panc-1 cells, both observations consistent with differential RITC and TEM cellular uptake measurements in these same cell lines.

Gemcitabine Release Studies

The gemcitabine loading efficiency of these c(RGDfE)-pMMSNs was as high as 75% (GEM loading amount ×100%／GEM total amount, 4.75 mg GEM / 1 mg RGD-pMMSNs). The gemcitabine release curve for loaded c(RGDfE)-pMMSNs is shown in **Fig. 6a**. A typical two-phase drug release profile was observed with 40% of the loaded gemcitabine released within the first 8 hours, 40% released during sustained phase from 8-72 hours; overall 90% of the gemcitabine was released within 72 hours (**Fig. 6a**).

In vitro Biocompatibility and Therapeutic Efficacy

The cytotoxicity of pMMSNs was evaluated for BxPC-3, CFPAC-1, Panc-1 cell lines with MTT assay. Cell viability remained above 80% even upon exposure to high concentration of 100 μg/ml (**Fig. 6b**), indicating the good biocompatibility of these pMMSNs. The half-maximum inhibition concentration (IC_{50} value) of free gemcitabine was evaluated in BxPC-3, Panc-1, CFPAC-1 cell lines (**Fig. 6c**). The IC_{50} values for gemcitabine in 0.106 μM, 0.064 μM and 18.480 μM for BxPC-3, CFPAC-1, and Panc-1, respectively. To evaluate the therapeutic efficacy of c(RGDfE)-pMMSNs loaded with gemcitabine, three different intervals (1h, 8h and 24h) were chosen for exposure periods with the three cell lines (**Fig. 6d**). For BxPC-3 and CFPAC-1 lines, cell viability decreased with increasing exposure times ($p=0.0005$, 0.0013 respectively), while there was no significant decrease observed among the three different intervals in Panc-1 cells ($p = 0.7$). Further data analysis showed that the viable decreases were significant across the three intervals in the BxPC-3 cells ($p < 0.05$). For the CFPAC-1 cells, viability decreases between 8 h and 24 h exposure periods were not found statistically significant ($p>0.05$).

DISCUSSION

The prognosis for patients with pancreatic cancer is very poor with 5-year survival rates less than 6%.[1] Early metastasis and loco-regional recurrence occur in more than 80% of these patients.[2] Chemotherapy alone or in combination with other therapeutic approaches remains the preferred treatment for most patients with advanced pancreatic cancer. Since the first report by Burris et.al.,[9] gemcitabine has been used as the first-line therapeutic agent for advanced pancreatic cancer. However, gemcitabine chemotherapy and combined chemotherapy with therapeutic agents including fluorouracil[51], capecitabine,[52, 53] cisplatin,[54] irinotecan,[55] oxaliplatin,[56] have shown minimal improvements in 5-year survival rates. Non-specific delivery of these therapeutic agents, chemo-resistance of pancreatic cancer, insufficient drug concentrations reaching the tumors and side effects that limit overall dose during systemic administration are each critical factors negatively impacting therapeutic efficacy. There is an urgent need to develop an effective and efficient targeted drug delivery system to increase the local tumor drug concentrations. In this study, we designed a targeted drug delivery system based upon the multi-functional nanoparticles [c(RGDfE)-pMMSNs]. We selected the c(RGDfE) peptide as the targeting probe with high binding affinity to integrin $\alpha_v\beta_3$ overexpressed in human pancreatic cancer cells. The selective uptake of these nanoparticles should be dependent upon

the integrin expression levels of the targeted cancer cells. The results of our study showed that c(RGDfE) conjugated pMMSNs were more effectively internalized by BXPC-3 pancreatic cancer cells that demonstrated higher integrin $\alpha_v\beta_3$ expression levels that permitted enhanced cellular uptake via receptor-mediated endocytosis. Gemcitabine release from these c(RGDfE)-pMMSNs was able to inhibited pancreatic cancer cell growth. The MNCs in the core of these nanoparticles eliciting strong MRI contrast to potentially permit non-invasive monitoring of c(RGDfE)-pMMSNs delivery for early prediction of treatment outcomes.

The synthesized MNCs were highly water dispersible and stable at RT. These 24 nm MNCs demonstrated stronger MRI relaxivity than commercial SPIOs of similar sizes (17-31nm). The high relaxivity and super-paramagnetic properties of these MNCs should permit these to serve as excellent *in vivo* MRI contrast agents.[57] To provide capacity for gemcitabine drug loading, the MNCs were further modified with an amine terminated mesoporous silica shell (MMSNs). Thus, the surface of these MMSNs could be conjugated with targeting molecules c(RGDfE) peptides. To form the mesostructured silica shell, CTAB was used as the templates, which was removed later to form pores on the shell. The 2-3 nm pores generated provide a large internal space for drug loading. Amine terminated surface was caused by APTMS modification and the pMMSNs were further capped with PEG molecules which for conjugation with c(RGDfE) peptides. This PEG modification should also reduce the nonspecific uptake of the nanoparticles by the RES and increase circulation time *in vivo*.[58, 59]

To achieve targeting delivery of the pMMSNs to pancreatic cancer cells, c(RGDfE) peptides were selected as the targeting probe. These c(RGDfE) peptide grafted pMMSNs (RGD-pMMSNs) can bind to the integrin $\alpha_v\beta_3$ which is over expressed upon many different types of tumor cells.[39, 41] This binding should permit c(RGDfE) -pMMSNs to be taken into the tumor cells via receptor-mediated endocytosis.[28] Subsequently intra-cellular gemcitabine release will occur after the internalization, which should lead to cell death. TEM results showed that most of the internalized c(RGDfE)-pMMSNs accumulated around the nucleus. This result is consistent with the prior studies.[41, 60] The cellular uptake in three different pancreatic cancer cell lines was compared with IF imaging. Cellular uptake was related to the expression level of integrin $\alpha_v\beta_3$, which indicates that the uptake was most likely due to integrin-mediated endocytosis. While not included in current studies, a free c(RGDfE) peptide blocking group could be valuable for future studies providing additional validation of the specific mechanism for selective c(RGDfE)-pMMSN delivery.

Gemcitabine, which is used as a standard therapeutic for pancreatic cancer, is a nucleoside analogue and should induce cell apoptosis via interfering with the process of DNA replication.[61] Given the drug's mechanism of action, c(RGDfE)-pMMSNs accumulation near the nucleus (observed during TEM) should thus be highly serendipitous. *In vitro* drug release studies showed that there were two phases of the gemcitabine release. In the first 8 hours, the release was fast and almost 50% of the loaded gemcitabine was released. Then the release rate slowed with a sustained release rate observed for roughly three days during which remaining 40% of initially loaded drug dose was released. Initially the 10% of gemcitabine drug released during first hour showed minimal impact upon the growth rate of the exposed cells. However, longer incubation times allowed a greater amount of the gemcitabine to be released, thus eliciting a time dependent pattern of cell growth inhibition, particularly for the BxPC-3 cell line. The increasing incubation time from 1h to 8 h and 24 h decreased the viability of BxPC-3 cells. However, while significant decreases of CFPAC-1 cell viabilities were observed at 8 and 24 h when compared to 1 h of c(RGDfE)-pMMSN exposure, CFPAC-1 and PANC-1 cell lines did show significant time dependent decreases between the 8 h and 24 h time intervals, likely due to the lower expression levels of integrin $\alpha_v\beta_3$ in these two cell lines (CFPAC-1 and PANC-1). For the cell line PANC-1, no significant differences were observed in cell viability at any of the follow-up exposure periods. This was likely due to the relatively low sensitivity to gemcitabine for PANC-1 cell lines (IC_{50}: 18.5 μM). After the first hour of exposure, only roughly 10% of gemcitabine would be released. Even at the 24 h incubation (0.3799 μM gemcitabine released), cell viability remained above 80%. Further, expression of integrin $\alpha_v\beta_3$ was lower in these PANC-1 cells, thus endocytosis was likely not enhanced with increased incubation times.

CONCLUSION

We developed c(RGDfE) peptides-grafted magnetic mesoporous silica nanoparticles for the purpose of target delivery of gemcitabine to pancreatic cancer cells. Included magnetic components at the core of the drug carriers produce strong MR contrast effects to facilitate non-invasive monitoring of the delivery of these drug carriers and tumors. c(RGDfE) peptides conjugation to these magnetic drug carriers achieved specific binding to pancreatic cancer cells for targeted drug delivery to enhance anticancer effects with intra-cellular release of gemcitabine. This efficient multi-functional magnetic drug delivery system has the potential for application as a new approach for targeted pancreatic cancer therapy.

ACKNOWLEDGMENTS

The author reports no conflicts of interest in this work.

Grant Support: This work was supported by the National Key Basic Research Program of the PRC (2014CB744500, 2011CB707700), the Major International (Regional) Joint Research Program of China (81120108013) and the National Science Foundation of China (NSFC) (30930028, 81101039, 81322020, 81230032, 81171313 and 81401469). Thanks the China Scholarship Council (CSC) for the financial support.

Figures

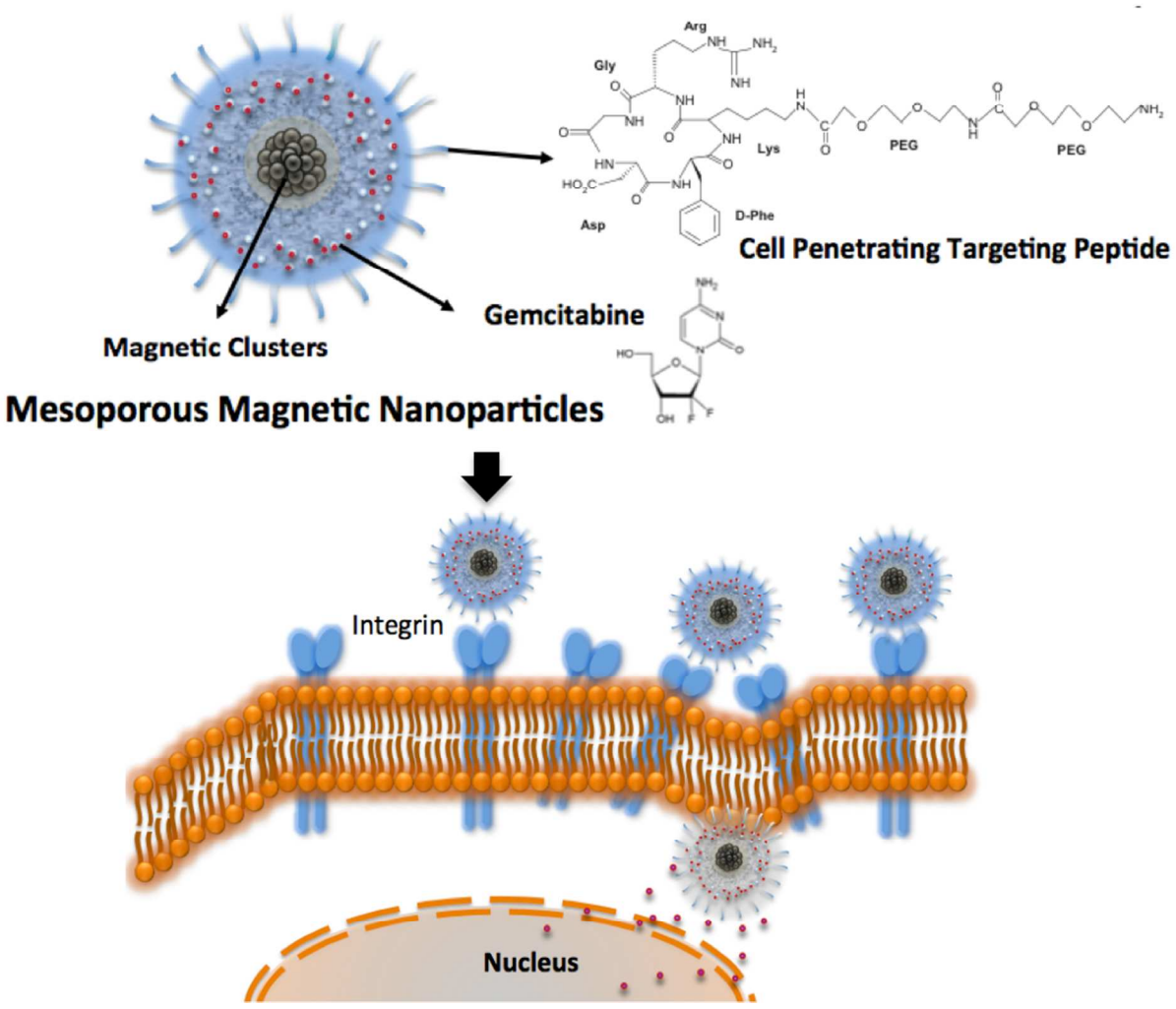

Figure 1. Schematic of targeted gemcitabine drug delivery using c(RGDfE) peptide-magnetic mesoporous silica nanoparticles [c(RGDfE)-pMMSNs].

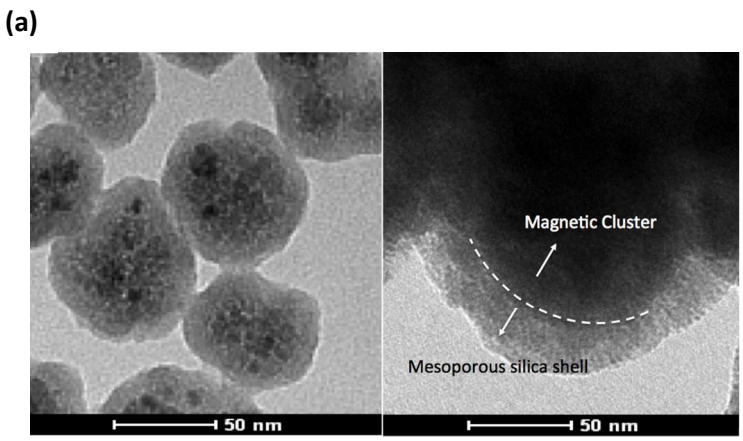

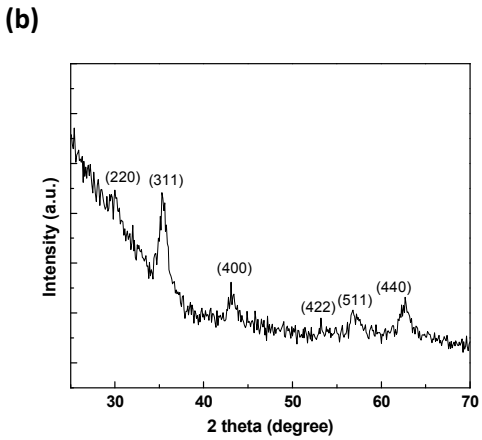

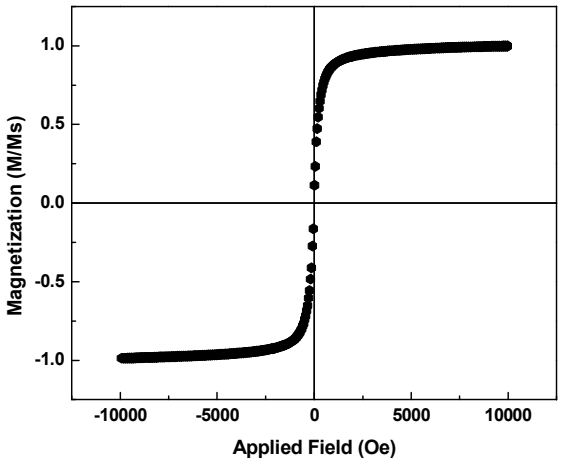

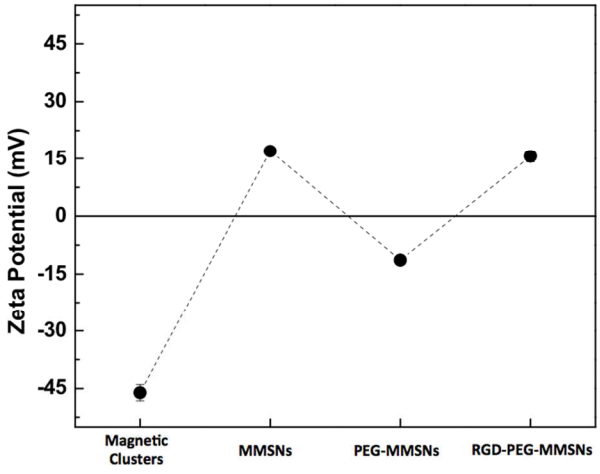

Figure 2. (**a**) HR-TEM images of magnetic mesoporous silica nanoparticles (pMMSNs) showing structure of magnetic cluster core and mesoporous silica shell (right panel). (**b**) X-Ray diffraction (XRD) data for pMMSNs. (**c**) Magnetization graph for pMMSNs at magnetic field application from −10 kOe to +10 kOe. (**d**) Zetapotential changes for each nanoparticle surface modifications.

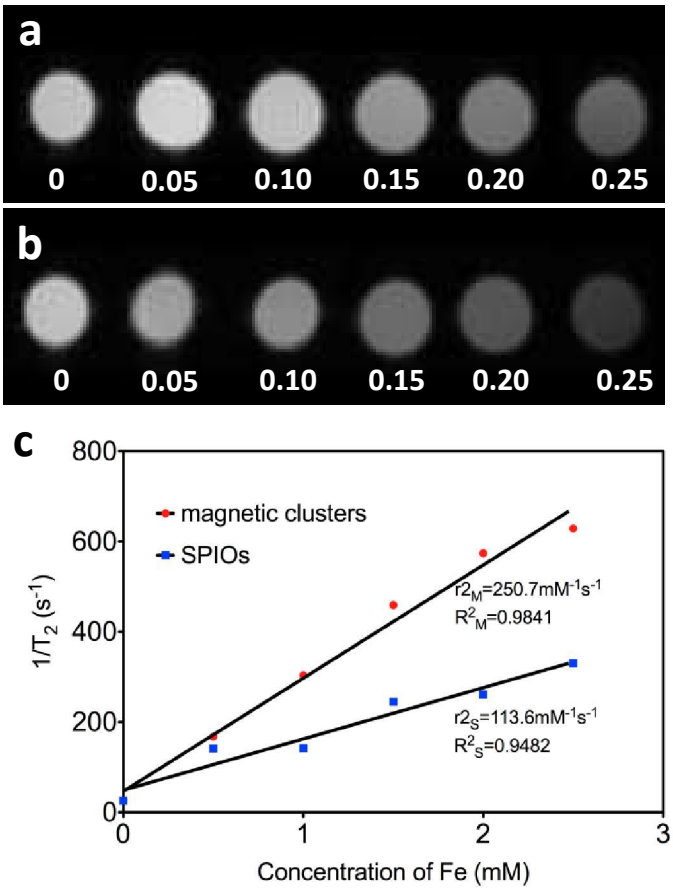

Figure 3. T_2 weighted MRI images (**a**, **b**), R_2 (= $1/T_2$) values and relaxivities (**c**) of phantoms containing increasing concentrations of commercial SPIOs (**a**) and our synthesized magnetite nanoclusters (**b**).

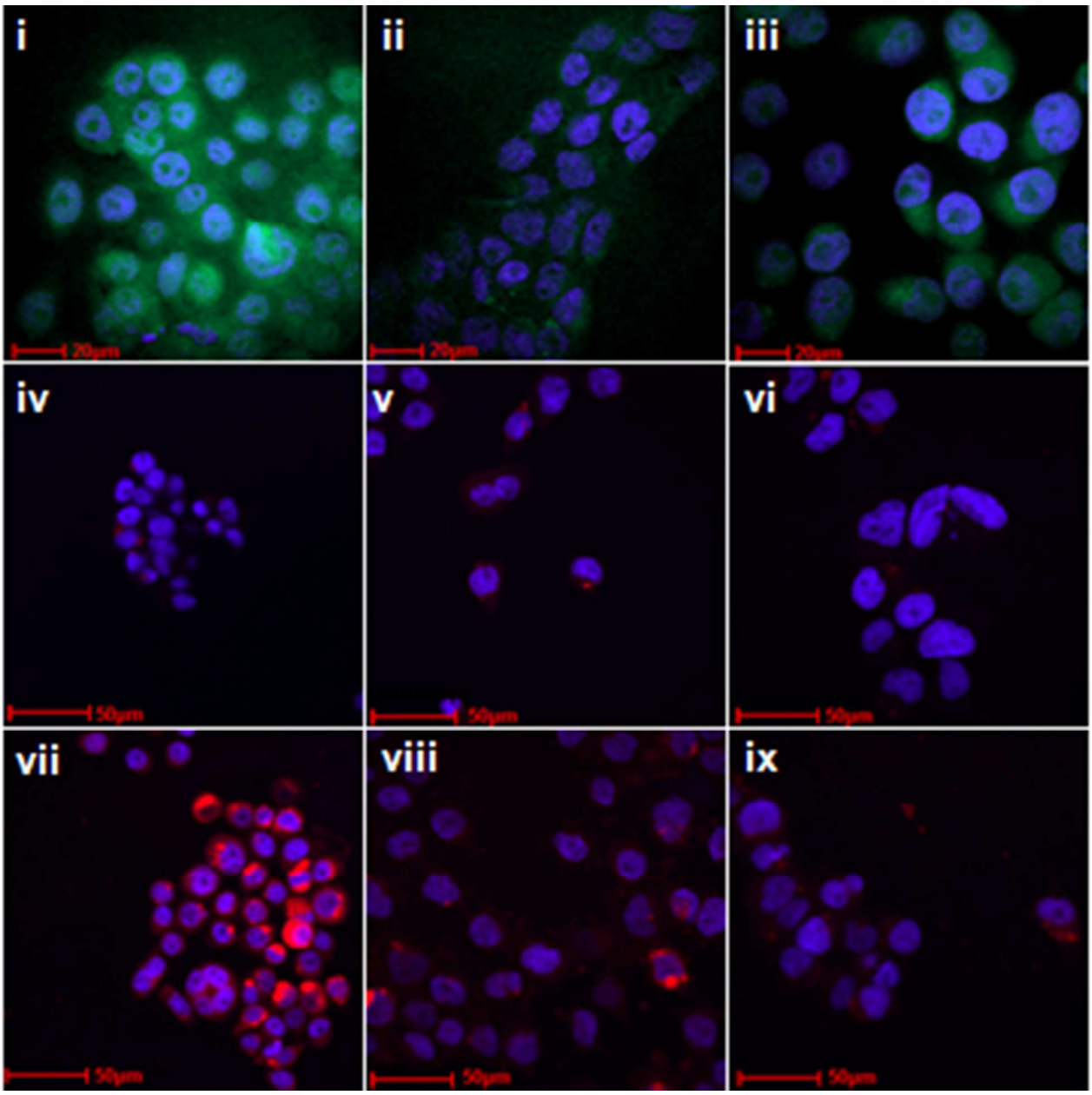

Figure 4. Intravital fluorescence imaging of the expression of integrin $\alpha_v\beta_3$ in three different human pancreatic cancer cell lines BxPC-3 (**i**), CFPAC-1 (**ii**), Panc-1 (**iii**). Cellular uptake of RITC labeled pMMSNs and c(RGDfE)-pMMSNs in BxPC-3 (**iv**, **vii**), CFPAC-1 (**v**, **viii**), Panc-1 (**vi**, **ix**).

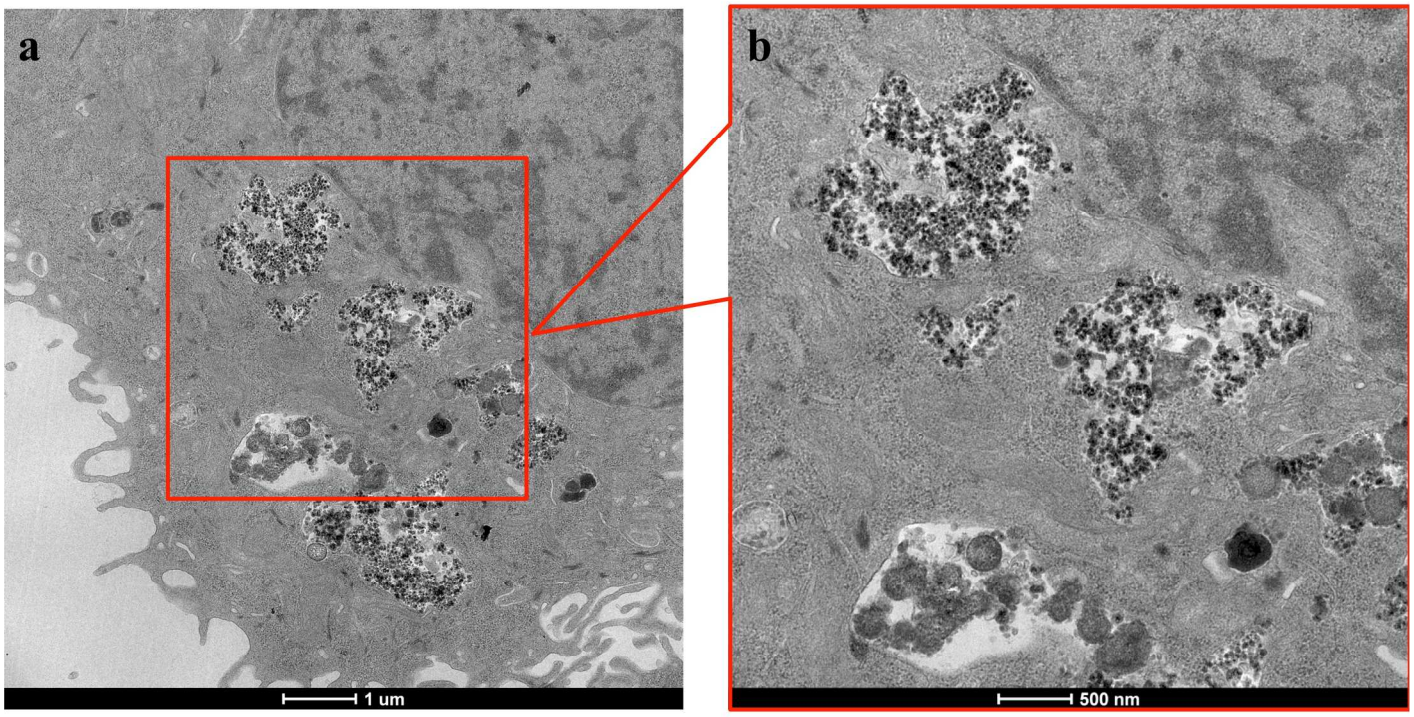

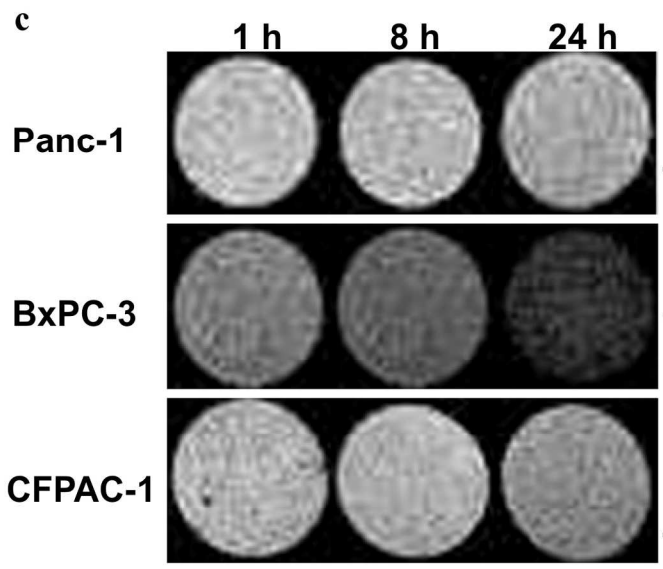

	Signal intensity		
	1 hour	8 hour	24 hour
Panc-1	369.6±26.7	357.4±22.7	343.5±25.4
BxPC-3	271.7±25.1	253.3±26.1	134.8±23.7
CFPAC-1	352.7±33.7	347.8±24.1	285.3±26.8

Figure 5. TEM and MR images of the cellular uptake of c(RGDfE)-pMMSNs in human pancreatic cancer cells. (**a**) A large number of nanoparticles aggregated around the nucleus of BXPC-3 cells. (**b**) High magnification TEM image of the red inset area in (**a**). (c) T_2 weighted MR images of three different pancreatic cancer cell suspension phantoms (Panc-1, BxPC-3 and CFPAC-1) after incubation with c(RGDfE)-pMMSNs for 1, 8 and 24 hours along with associated signal intensity measurements.

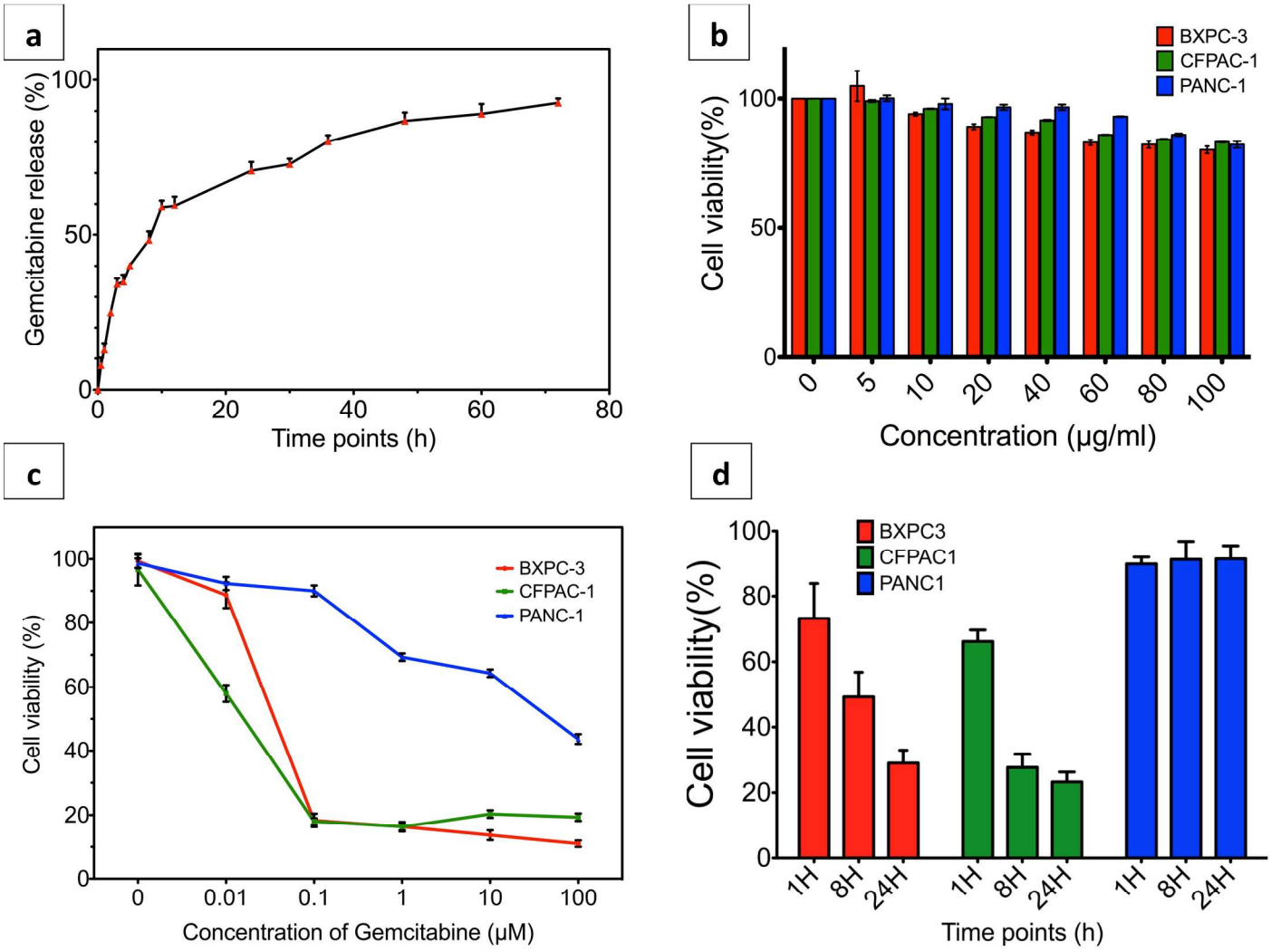

Figure 6. (a) *In vitro* study of gemcitabine release from c(RGDfE)-pMMSNs. At 1 hour, less than 10% of gemcitabine was released from the particles. At 8 hour, almost 50% of the gemcitabine was released. 90% of gemcitabine was released at 60 hours. (b) Cytotoxicity of c(RGDfE)-pMMSNs in three pancreatic cancer cell lines. (c) Gemcitabine dosage dependent cell viability in three different human pancreatic cancer cell lines (BxPC-3, CFPAC-1 and Panc-1). (d) Comparison of therapeutic effects on the three cell lines incubated with c(RGDfE)-pMMSNs loading with gemcitabine for different time intervals (1h, 8h, 24h).

Reference

1. R. Siegel, D. Naishadham and A. Jemal, *CA Cancer J. Clin.*, 2013, **63**, 11-30.
2. A. S. Paulson, H. S. Tran Cao, M. A. Tempero and A. M. Lowy, *Gastroenterology*, 2013, **144**, 1316-1326.
3. J. P. Neoptolemos, D. D. Stocken, H. Friess, C. Bassi, J. A. Dunn, H. Hickey, H. Beger, L. Fernandez-Cruz, C. Dervenis, F. Lacaine, M. Falconi, P. Pederzoli, A. Pap, D. Spooner, D. J. Kerr, M. W. Buchler and C. European Study Group for Pancreatic, *N. Engl. J. Med.*, 2004, **350**, 1200-1210.
4. J. P. Neoptolemos, M. J. Moore, T. F. Cox, J. W. Valle, D. H. Palmer, A. C. McDonald, R. Carter, N. C. Tebbutt, C. Dervenis, D. Smith, B. Glimelius, R. M. Charnley, F. Lacaine, A. G. Scarfe, M. R. Middleton, A. Anthoney, P. Ghaneh, C. M. Halloran, M. M. Lerch, A. Olah, C. L. Rawcliffe, C. S. Verbeke, F. Campbell, M. W. Buchler and C. European Study Group for Pancreatic, *JAMA*, 2012, **308**, 147-156.
5. H. Oettle, S. Post, P. Neuhaus, K. Gellert, J. Langrehr, K. Ridwelski, H. Schramm, J. Fahlke, C. Zuelke, C. Burkart, K. Gutberlet, E. Kettner, H. Schmalenberg, K. Weigang-Koehler, W. O. Bechstein, M. Niedergethmann, I. Schmidt-Wolf, L. Roll, B. Doerken and H. Riess, *JAMA*, 2007, **297**, 267-277.
6. S. Boeck, D. P. Ankerst and V. Heinemann, *Oncology*, 2007, **72**, 314-321.
7. P. Maisonneuve and A. B. Lowenfels, *JAMA*, 2007, **297**, 2581; author reply 2582.
8. F. Ren, Y. C. Xu, H. X. Wang, L. Tang and Y. Ma, *Pancreatology*, 2012, **12**, 162-169.
9. H. A. Burris, 3rd, M. J. Moore, J. Andersen, M. R. Green, M. L. Rothenberg, M. R. Modiano, M. C. Cripps, R. K. Portenoy, A. M. Storniolo, P. Tarassoff, R. Nelson, F. A. Dorr, C. D. Stephens and D. D. Von Hoff, *J. Clin. Oncol.*, 1997, **15**, 2403-2413.
10. V. Heinemann, D. Quietzsch, F. Gieseler, M. Gonnermann, H. Schönekäs, A. Rost, H. Neuhaus, C. Haag, M. Clemens and B. Heinrich, *J. Clin. Oncol.*, 2006, **24**, 3946-3952.
11. J. D. Berlin, P. Catalano, J. P. Thomas, J. W. Kugler and D. G. Haller, *J. Clin. Oncol.*, 2002, **20**, 3270-3275.
12. C. Louvet, R. Labianca, P. Hammel, G. Lledo, M. Zampino, T. Andre, A. Zaniboni, M. Ducreux, E. Aitini and J. Taieb, *J. Clin. Oncol.*, 2005, **23**, 3509-3516.
13. R. Herrmann, G. Bodoky, T. Ruhstaller, B. Glimelius, E. Bajetta, J. Schüller, P. Saletti, J. Bauer, A. Figer and B. Pestalozzi, *J. Clin. Oncol.*, 2007, **25**, 2212-2217.
14. E. Van Cutsem, W. L. Vervenne, J. Bennouna, Y. Humblet, S. Gill, J.-L. Van Laethem, C. Verslype, W. Scheithauer, A. Shang and J. Cosaert, *J. Clin. Oncol.*, 2009, **27**, 2231-2237.
15. G. Y. Lee, W. P. Qian, L. Wang, Y. A. Wang, C. A. Staley, M. Satpathy, S. Nie, H. Mao and L. Yang, *ACS nano*, 2013, **7**, 2078-2089.
16. S. A. Mackowiak, A. Schmidt, V. Weiss, C. Argyo, C. von Schirnding, T. Bein and C. Bräuchle, *Nano lett.*, 2013, **13**, 2576-2583.
17. H. Meng, Y. Zhao, J. Dong, M. Xue, Y.-S. Lin, Z. Ji, W. X. Mai, H. Zhang, C. H. Chang and C. J. Brinker, *ACS nano*, 2013, **7**, 10048-10065.
18. A.-L. Papa, S. Basu, P. Sengupta, D. Banerjee, S. Sengupta and R. Harfouche, *BMC cancer*, 2012, **12**, 419.

19. K. Yokoi, B. Godin, C. J. Oborn, J. F. Alexander, X. Liu, I. J. Fidler and M. Ferrari, *Cancer lett.*, 2013, **334**, 319-327.
20. S.-r. Ji, C. Liu, B. Zhang, F. Yang, J. Xu, J. Long, C. Jin, D.-l. Fu, Q.-x. Ni and X.-j. Yu, *BBA-REV CANCER*, 2010, **1806**, 29-35.
21. Y. Malam, M. Loizidou and A. M. Seifalian, *Trends Pharmacol. Sci.*, 2009, **30**, 592-599.
22. C. R. Patra, R. Bhattacharya, D. Mukhopadhyay and P. Mukherjee, *Adv. Drug Deliv. Rev.*, 2010, **62**, 346-361.
23. S. Prakash, M. Malhotra, W. Shao, C. Tomaro-Duchesneau and S. Abbasi, *Adv. Drug Deliv. Rev.*, 2011, **63**, 1340-1351.
24. F. Yang, C. Jin, Y. Jiang, J. Li, Y. Di, Q. Ni and D. Fu, *Cancer Treat. Rev.*, 2011, **37**, 633-642.
25. F. Yang, C. Jin, S. Subedi, C. L. Lee, Q. Wang, Y. Jiang, J. Li, Y. Di and D. Fu, *Cancer Treat. Rev.*, 2012, **38**, 566-579.
26. Z. Zhou, H. Chen, M. Lipowska, L. Wang, Q. Yu, X. Yang, D. Tiwari, L. Yang and H. Mao, *J. Biomater. Appl.*, 2013, **28**, 100-111.
27. F. Zhang, G. B. Braun, A. Pallaoro, Y. Zhang, Y. Shi, D. Cui, M. Moskovits, D. Zhao and G. D. Stucky, *Nano lett.*, 2012, **12**, 61-67.
28. F. Tang, L. Li and D. Chen, *Adv. Mater.*, 2012, **24**, 1504-1534.
29. J. Yang, F. Zhang, W. Li, D. Gu, D. Shen, J. Fan, W. X. Zhang and D. Zhao, *Chem. Commun. (Camb)*, 2014, **50**, 713-715.
30. H.-L. Tu, Y.-S. Lin, H.-Y. Lin, Y. Hung, L.-W. Lo, Y.-F. Chen and C.-Y. Mou, *Adv. Mater.*, 2009, **21**, 172-177.
31. B. Chang, J. Guo, C. Liu, J. Qian and W. Yang, *J. Mater. Chem.*, 2010, **20**, 9941.
32. M. F. Y. T. Nawal Kishor Mal, *Nature*, 2003, **421**, 347-350.
33. J. L. Vivero-Escoto, I. I. Slowing, C.-W. Wu and V. S.-Y. Lin, *J. Am. Chem. Soc.*, 2009, **131**, 3462-3463.
34. A. Popat, J. Liu, G. Q. Lu and S. Z. Qiao, *J. Mater. Chem.*, 2012, **22**, 11173.
35. L. Xing, H. Zheng, Y. Cao and S. Che, *Adv. Mater.*, 2012, **24**, 6433-6437.
36. S. Y. Park, Y. Lee, K. H. Bae, C.-H. Ahn and T. G. Park, *Macromol. Rapid Commun.*, 2007, **28**, 1172-1176.
37. A. Bernardos, E. Aznar, M. D. Marcos, R. Martinez-Manez, F. Sancenon, J. Soto, J. M. Barat and P. Amoros, *Angew. Chem. Int. Ed. Engl.*, 2009, **48**, 5884-5887.
38. M. L. Bernardos A, Aznar E, Marcos MD, Martinez-Mañez R, Sancenon F, Soto J, Barat JM, Perez-Paya E, Guillem C, Amoros P, *ACS nano*, 2010, **4**, 6353-6368.
39. H. M. Sheldrake and L. H. Patterson, *Curr. Cancer Drug Targets*, 2009, **9**, 519-540.
40. R. Hosotani, M. Kawaguchi, T. Masui, T. Koshiba, J. Ida, K. Fujimoto, M. Wada, R. Doi and M. Imamura, *Pancreas*, 2002, **25**, e30-35.
41. J. S. Desgrosellier and D. A. Cheresh, *Nat. Rev. Cancer*, 2010, **10**, 9-22.
42. J. H. Lee, K. Lee, S. H. Moon, Y. Lee, T. G. Park and J. Cheon, *Angew. Chem. Int. Ed. Engl.*, 2009, **48**, 4174-4179.

43. X. B. Xiong, A. Mahmud, H. Uludag and A. Lavasanifar, *Pharm. Res.*, 2008, **25**, 2555-2566.
44. N. Nasongkla, E. Bey, J. Ren, H. Ai, C. Khemtong, J. S. Guthi, S. F. Chin, A. D. Sherry, D. A. Boothman and J. Gao, *Nano lett.*, 2006, **6**, 2427-2430.
45. K. Temming, R. M. Schiffelers, G. Molema and R. J. Kok, *Drug Resist. Updat.*, 2005, **8**, 381-402.
46. S. Liu, *Bioconjug. Chem.*, 2009, **20**, 2199-2213.
47. S. Liu, *Mol. Pharm.*, 2006, **3**, 472-487.
48. J. Ge, Y. Hu, M. Biasini, W. P. Beyermann and Y. Yin, *Angew. Chem. Int. Ed. Engl.*, 2007, **46**, 4342-4345.
49. Y. G. Dong-Hyun Kim, Zhuoli Zhang, Daniel Procissi, Jodi Nicolai, Reed A. Omary, Andrew C. Larson,, *Adv. Healthc. Mater.*, 2013, **In press**.
50. D.-H. Kim, Y. Guo, Z. Zhang, D. Procissi, J. Nicolai, R. A. Omary and A. C. Larson, *Adv. Healthc. Mater.*, 2013, n/a-n/a.
51. J. D. Berlin, P. Catalano, J. P. Thomas, J. W. Kugler, D. G. Haller and A. B. Benson, 3rd, *J. Clin. Oncol.*, 2002, **20**, 3270-3275.
52. R. Herrmann, G. Bodoky, T. Ruhstaller, B. Glimelius, E. Bajetta, J. Schuller, P. Saletti, J. Bauer, A. Figer, B. Pestalozzi, C. H. Kohne, W. Mingrone, S. M. Stemmer, K. Tamas, G. V. Kornek, D. Koeberle, S. Cina, J. Bernhard, D. Dietrich, W. Scheithauer, R. Swiss Group for Clinical Cancer and G. Central European Cooperative Oncology, *J. Clin. Oncol.*, 2007, **25**, 2212-2217.
53. D. Cunningham, I. Chau, D. D. Stocken, J. W. Valle, D. Smith, W. Steward, P. G. Harper, J. Dunn, C. Tudur-Smith, J. West, S. Falk, A. Crellin, F. Adab, J. Thompson, P. Leonard, J. Ostrowski, M. Eatock, W. Scheithauer, R. Herrmann and J. P. Neoptolemos, *J. Clin. Oncol.*, 2009, **27**, 5513-5518.
54. G. Colucci, R. Labianca, F. Di Costanzo, V. Gebbia, G. Carteni, B. Massidda, E. Dapretto, L. Manzione, E. Piazza, M. Sannicolo, M. Ciaparrone, L. Cavanna, F. Giuliani, E. Maiello, A. Testa, P. Pederzoli, M. Falconi, C. Gallo, M. Di Maio, F. Perrone, M. Gruppo Oncologico Italia, D. Gruppo Italiano per lo Studio dei Carcinomi dell'Apparato and C. Gruppo Oncologico Italiano di Ricerca, *J. Clin. Oncol.*, 2010, **28**, 1645-1651.
55. G. P. Stathopoulos, K. Syrigos, G. Aravantinos, A. Polyzos, P. Papakotoulas, G. Fountzilas, A. Potamianou, N. Ziras, J. Boukovinas, J. Varthalitis, N. Androulakis, A. Kotsakis, G. Samonis and V. Georgoulias, *Br. J. Cancer*, 2006, **95**, 587-592.
56. E. Poplin, Y. Feng, J. Berlin, M. L. Rothenberg, H. Hochster, E. Mitchell, S. Alberts, P. O'Dwyer, D. Haller, P. Catalano, D. Cella and A. B. Benson, 3rd, *J. Clin. Oncol.*, 2009, **27**, 3778-3785.
57. G. Liu, J. Gao, H. Ai and X. Chen, *Small*, 2013, **9**, 1533-1545.
58. J. V. Jokerst, T. Lobovkina, R. N. Zare and S. S. Gambhir, *Nanomedicine*, 2011, **6**, 715-728.
59. D. Liu, W. Wu, J. Ling, S. Wen, N. Gu and X. Zhang, *Adv. Funct. Mater.*, 2011, **21**, 1498-1504.
60. F. Danhier, V. Pourcelle, J. Marchand-Brynaert, C. Jerome, O. Feron and V. Preat, *Methods Enzymol.*, 2012, **508**, 157-175.
61. N. M. Cerqueira, P. A. Fernandes and M. J. Ramos, *Chemistry*, 2007, **13**, 8507-8515.